Compatibilization of Polymer Blends by Complexation. 2. Kinetics of Interfacial Mixing

Yi Feng,[†,‡] R. A. Weiss,[*,†] Alamgir Karim,[§] C. C. Han,[§] John F. Ankner,[⊥] Helmut Kaiser,[⊥] and Dennis G. Peiffer[∥]

Institute of Materials Science, University of Connecticut, Storrs, Connecticut 06269-3136, Polymers Division, National Institute of Standards and Technology, Gaithersburg, Maryland 20899, Reactor Research Facility, University of Missouri−Columbia, Columbia, Missouri 65211, and Corporate Research Laboratory, Exxon Research & Engineering Company, Route 22 East, Clinton Township, Annandale, New Jersey 08801

Received November 20, 1995; Revised Manuscript Received March 12, 1996[⊗]

ABSTRACT: The interfacial composition and kinetics of interfacial mixing of two polymers that exhibit strong exothermic interactions, poly(*N*,*N*′-dimethylethylenesebacamide) (mPA) and the lithium salt of a lightly sulfonated polystyrene ionomer containing 7.4 mol % sulfonate groups (Li−SPS), were characterized by neutron reflectivity measurements. Blends of Li−SPS and mPA are miscible below ca. 150 °C as a result of the formation of an ion−dipole complex between the Li^+−sulfonate and amide groups. Neutron reflectivity measurements were carried out on spun-coated bilayer films of the polyamide and a deuterated sample of the ionomer. The films were annealed at 96 °C, which is above the melting temperature of the mPA (T_m = 75 °C) but below the glass transition temperature of the ionomer (T_g = 120 °C). The interface between the two films exhibited an asymmetric concentration profile due to the large viscosity mismatch between the two polymer, and the interfacial mixing followed neither Fickian nor Case II diffusion. A kinetic model that combined Fickian diffusion with a suppression of mobility due to intermolecular cross-linking adequately represented the experimental data.

Introduction

The development of strong specific interactions or complexation between two different polymers is a subject that has attracted considerable interest over the past decade.[1−8] These complexes not only provide a viable method for compatibilizing multicomponent polymer mixtures to attain tailored properties[9,10] but they also offer new challenges for fundamental studies of interfacial phenomena.[11,12] Interfacial mixing in polymer blends results from interdiffusion of the different components, which governs the interfacial width and composition profile at the interface. The amount of interfacial mixing that occurs in a blend influences the morphology and interfacial adhesion, which ultimately control the physical and mechanical properties of the blend.

Interfacial mixing begins when two polymer surfaces are brought into contact,[13] and the extent and rate of interdiffusion depend on the interactions between the two polymers.[14] General theories regarding polymer interdiffusion and the techniques used to study polymer−polymer interfacial mixing and measure diffusion coefficients are described in two recent reviews.[11,12] This paper considers the evolution of the interfacial composition profile and the displacement of the interface during interfacial mixing of a polymer pair with a large mismatch in their respective molecular mobilities and for which strong exothermic, intermolecular interactions occur.

Diffusion of low molecular weight species is usually *Fickian* with a constant diffusion coefficient.[15] For polymer solutions or melts where both components are relatively mobile, interdiffusion is Fickian but with a concentration-dependent diffusion coefficient. As a result, the interface moves linearly with respect to the square root of time in the direction of the species with the higher mobility.[16−20]

Transport in glassy polymers cannot generally be described by Fickian diffusion.[21] In that case, diffusion is influenced by the relaxation times of the glassy polymer, and the combined process of molecular relaxation and diffusion is called "anomalous diffusion". In the limiting case when the transport rate is dominated by polymer relaxation, the process is designated "Case II diffusion".[22] A characteristic feature of Case II diffusion is that as the mobile species penetrates into the glassy polymer, a sharp advancing boundary separating the inner glassy core from the outer swollen rubbery shell moves at a constant velocity toward the glassy polymer. Case II diffusion has been generally observed for the sorption of organic solvents into polymer glasses.[22−26] Interdiffusion of a polymer−polymer mixture in which one of the components was a glass, poly(vinyl methyl ether)/polystyrene (PVME/PS) below the glass transition temperature of the polystyrene, was also shown to follow the Case II mechanism.[27,28]

In all prior studies of interdiffusion in polymer mixtures, the mobilities of the individual component polymers were relatively independent. The intermolecular forces between the different polymers were relatively weak, i.e., van der Waals forces or, for partially miscible polymer pairs such as PVME/PS, weak dipolar interactions. When the two diffusing polymers can form a molecular complex, however, one might expect a suppression of the interdiffusion process, especially when the intermolecular interactions are especially strong. In the extreme case where a physical network may form, mixing may stop completely because of the lack of molecular mobility as a result of network

* To whom correspondence should be sent.
† University of Connecticut.
‡ Current address: AT&T Bell Laboratories, 600 Mountain Avenue, Murray Hill, NJ 07974-0636.
§ National Institute of Standards & Technology.
⊥ University of Missouri−Columbia.
∥ Exxon Research & Engineering Co.
⊗ Abstract published in *Advance ACS Abstracts,* May 1, 1996.

S0024-9297(95)01723-2 CCC: $12.00

Table 1. Polymer Samples

Polymer	$10^{-3}M_n$, g/mol	$10^{-3}M_w$, g/mol	Tg, °C	density, g/cm^3	$10^6 b/V$, Å^{-2}
mPA	25	65	0	1.278[a]	0.788[d]
d-PS	100	107	100	1.116[b]	6.39[d]
d-LiSPS	106	114	120	1.17[c]	6.39[d]

[a] Measured by a pycnometer using heptane at room temperature. [b] From ref 44. [c] Corrected for a deuterated ionomer using the results in ref 45. [d] Neutron scattering length density b/V was calculated from the elemental composition and the mass density.

formation at the interface. That situation would be analogous to superimposing on the diffusion process a cross-linking reaction so that extremely high molecular weight polymer is trapped at the interface between the two components. In that case, the kinetics of interdiffusion will be influenced not only by the binary diffusion coefficient but also by the kinetics of the cross-linking reaction.

The research described in this paper represents the first study in the kinetics of interfacial mixing where a strong intermolecular complex is formed upon mixing the two polymers. The polymers used were the lithium salt of a lightly sulfonated polystyrene ionomer and an *N*-methylated nylon 2, 10, i.e., poly(*N*,*N*′-dimethylethylenenesebacamide). The substitution of the methyl group for the amide proton prevented self-hydrogen bonding of the polyamide and provided a relatively low melting temperature, ca. 75 °C.[29] This provided the distinct advantage of having the melt state of the polyamide accessible at reasonable low experimental temperatures so that degradation of the polymers was not a crucial concern. The complexation between metal ions and amide groups has been previously documented for low molecular weight salts and secondary and tertiary amides.[30−33] Complexation of low molecular weight salts and polyamides has also been reported,[34,35] and ion−dipole interactions between the Li^+−sulfonate and the amide carbonyl oxygen have been confirmed in blends of Li−SPS with poly(ϵ-caprolactam)[36,37] and poly(*N*,*N*′-dimethylethylenesebacamide).[38,39]

A high-resolution technique is required to probe the interface between the polystyrene ionomer and the polyamide. In this study, neutron reflectivity was used since it provides subnanometer resolution and high contrast when one of the two polymer components is selectively deuterium−labeled.[40−42]

Experimental Section

Poly(*N*,*N*′-dimethylethylenesebacamide) was prepared by a nucleophilic acyl substitution reaction following the procedure of Huang and Kozakiewicz.[29] A 4 wt % *N*,*N*′-dimethylethylenediamine/tetrachloroethane solution containing 150% pyridine was added to an oven-dried, round-bottom, three-necked flask equipped with a gas inlet valve, a mechanical stirrer, and a stopper. The solution was cooled to ca. −15 °C, and a stoichiometric amount of sebacoyl chloride was added quickly while rapidly stirring the solution. The stirring was continued for about 24 h while the reaction mixture was allowed to gradually warm to room temperature under nitrogen. The resulting polymer was washed with water and then heptane. The number- and weight-average molecular weights measured in 1-methyl-2-pyrrolidinone at room temperature by gel permeation chromatography (GPC) were 25 000 and 65 000 g/mol, respectively. The properties of the *N*-methylated polyamide, hereafter referred to as mPA, are given in Table 1, and the molecular structure is shown below:

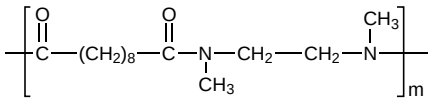

Deuterated polystyrene was prepared by anionic polymerization of styrene-d_8. The weight-average molecular weight was 107 000 g/mol and the polydispersity was 1.08 as measured by GPC. The sulfonation reaction was carried out in dichloroethane at ca. 50 °C using acetyl sulfate as the sulfonating reagent.[43] This particular reaction provides random substitution of sulfonic acid groups along the chain at the para position of the phenyl ring. The reaction was terminated by adding lithium acetate dissolved in a mixture of methanol and water, which also completely neutralized the sulfonic acid groups to Li^+−sulfonate groups. The deuterated ionomer, d-LiSPS, was then isolated by steam stripping and was dried under the vacuum at 100 °C for 24 h. The degree of sulfonation was 7.4 mol %, i.e., an average of 7.4 Li^+−sulfonate groups per 100 styrene repeat units, as calculated from the elemental sulfur concentration measured by Dietert sulfur analysis. The characteristics of the polymers used in this study are summarized in Table 1.

The specimen used for the interfacial mixing study was a bilayer film composed of a layer of mPA on top of a d-LiSPS layer cast on a silicon wafer. The d-LiSPS layer was prepared from a 1% d-LiSPS solution in a solvent mixture of 75/25 (v/v) methanol/tetrahydrofuran (THF) that was first filtered through a 0.45-μm PTFE filter and then spun cast at 2000 rpm onto a polished silicon disk. The silicon disks, obtained from Semiconductor Processing, Inc., were 10 cm in diameter with a surface roughness of ∼0.5 nm. Prior to spin coating, the silicon disk was cleaned in an acid bath of 70% H_2SO_4/30% H_2O_2 for 45 min at 80 °C, followed by thoroughly rinsing in deionized water. After spin coating, the homogeneous appearing thin d-LiSPS film was first air-dried and then dried in a vacuum oven for 30 min at 30 °C. A 1% solution of mPA in isopropyl alcohol, a nonsolvent for d-LiSPS, was then spun cast onto the d-LiSPS layer at 2000 rpm. The thickness of the mPA layer was estimated to be 72 nm from X-ray reflectivity measurements for a single-layer film spun cast onto a silicon disk under identical conditions.

Interfacial mixing was accomplished by placing the bilayer sample on a metal block heated to 96 °C (or 140 °C) and facing, but not in contact with, a second block heated to the same temperature in a vacuum oven for different periods of time. After the prescribed annealing period, the specimen was cooled to room temperature for the neutron reflectivity measurements. The sample temperature while in the oven was monitored by a bimetallic strip thermometer mounted in the sample heating block. For comparison, a single layer of d-LiSPS and a bilayer of mPA on top of d-PS were also prepared by using the same procedure described above, except that in the case of d-PS, a 1% solution of d-PS in THF was used.

The neutron reflectivity measurements were carried out at the Reactor Research Facility at the University of Missouri−Columbia. This instrument features a monochromatic beam (λ = 0.235 nm) used in an angle-dispersive configuration with a single ^{3}He detector. Data collection required a total of 3 h, which included a quasi-specular scan that was later subtracted from the raw specular data as a background correction. The principles of neutron reflectivity and the method used to analyze the experimental data can be found elsewhere.[40−42]

Results and Discussion

Interfacial Structure. Figure 1 shows a plot of the neutron reflectivity, R, as a function of neutron momentum normal to the film surface ($q = (2\pi/\lambda)\sin\theta$, where λ is the wavelength of the incident neutron beam and θ is the incident angle) for an as-coated film of d-LiSPS on a silicon substrate. The solid line represents the optimal reflectivity calculated by using a symmetric error function model[40,46] for the scattering length density profile at the interface. The choice of the function for fitting the air/polymer interface is arbitrary. Since typically the roughness of the air/polymer interface of spin-coated films is less than the instrument resolution of ∼1 nm, the precise choice of the functional form for

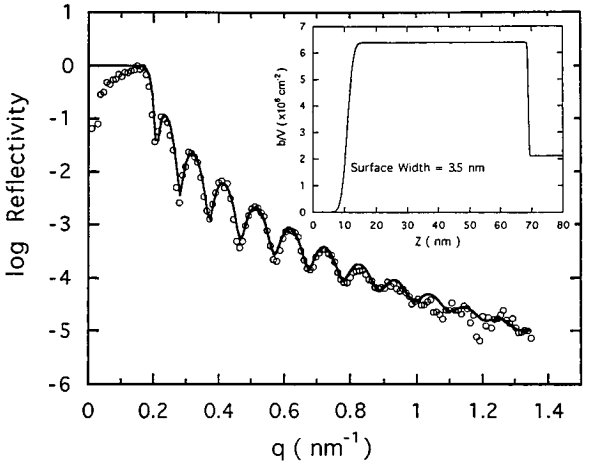

Figure 1. Neutron reflectivity from a single d-LiSPS layer on silicon substrate, as cast from solution. The solid line is the best fit using a symmetric interface model with a d-LiSPS layer thickness of 58 nm and an air/polymer interfacial roughness of 3.5 nm. This insert gives the profile of scattering length density as a function of the layer depth (Z), which was used to generate the solid line.

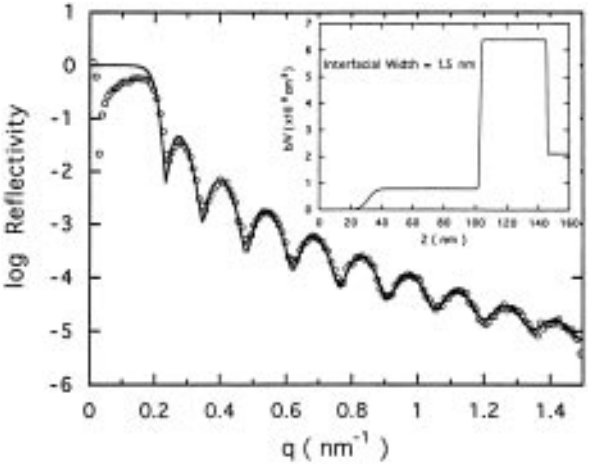

Figure 2. Neutron reflectivity from a mPA/d-PS bilayer on silicon annealed at 140 °C for 30 min. The solid line is the best fit using a d-PS layer thickness of 42.5 nm and a symmetric interface model with a polymer/polymer interfacial width of 1.5 nm. The insert gives the profile of scattering length density as a function of the layer depth (Z), which was used to generate the solid line. (The discrepancy between the solid line and the data at very small q is due to imperfections of the alignment at low q.)

that interface is not crucial. However, the complementary error function is a convenient starting profile for studying interdiffusion at the polymer/polymer interface, because it is the solution to the conventional Fickian diffusion problem.[15,41]

In the model, the first derivative of the scattering length density with respect to the depth Z is a Gaussian function,

$$G(Z) = \frac{\Delta(b/V)}{(2\Pi)^{1/2} Z_0} \exp\left(-\frac{Z^2}{2Z_0^2}\right) \qquad (1)$$

Here, $\Delta(b/V)$ is the scattering length density difference of the two bulk phases that form the interface, and Z_0 is the standard deviation of the Gaussian function that characterizes the interfacial width. The scattering length density, b/V (see Table 1), for d-LiSPS was calculated using the elemental composition of the polymer, tabulated values of the scattering lengths of each element, and the mass density of the polymer. This left only two adjustable parameters, the film thickness, d, and the air surface roughness or the air/polymer interfacial width, $\langle Z_0^2 \rangle^{1/2}$, for fitting the interface model to the experimental data. The best scattering length density profile fit, see insert in Figure 1, gave a film thickness of 58 nm and a surface roughness of 3.5 nm. Annealing the d-LiSPS film for 30 min at 140 °C did not change the magnitude of its air surface roughness. This fact is relevant to the interpretation of the interface broadening in the mPA/d-LiSPS bilayer upon annealing in that the broadening is due only to intermixing of the two polymers and not to other factors associated with a rearrangement of the d-LiSPS, e.g., dewetting of the lower layer. A neat d-PS layer on silicon has less air surface roughness, ca. 1.0 nm.[41]

Figure 2 shows the neutron reflectivity spectrum for a bilayer of mPA on top of d-PS after it was annealed at 140 °C for 30 min. The spectrum of the annealed sample was not noticeably different from the spectrum of the as-coated sample (not shown). The reflectivity from this bilayer film exhibits interference fringes characteristic of only a single 42.5-nm-thick d-PS layer. Two factors are responsible for this result. First, the neutron reflection is sensitive only to the mPA/d-PS (or d-LiSPS) interface and the d-PS (or d-LiSPS)/substrate interface. It is relatively insensitive to the mPA/Air interface, because the neutron scattering length density of mPA is only about one-eighth that of d-PS (or d-LiSPS); see Table 1. Second, although mPA does not self-hydrogen bond, it does slowly crystallize with time at room temperature. The neutron reflectivity measurements were performed at room temperature, and it typically took a few hours to get satisfactory statistics over the entire q range. During that period of time, a small amount of crystallization of the mPA may have occurred, which for reflectivity is equivalent to increasing the film surface roughness. X-ray reflectivity measurements on a single layer of mPA coated onto silicon under similar conditions gave a value for the air surface roughness of 10−15 nm, which for a bilayer would effectively smear out any X-ray or neutron reflectivity interference fringes resulting from the mPA layer. Those factors were actually advantageous with respect to the present study in that the large mismatch in the scattering length densities and the relatively high roughness at the mPA/air surface served to selectively highlight the film thickness of the d-PS (or d-LiSPS) layer and the interfacial width between mPA and d-PS (or d-LiSPS). The solid line in Figure 2 is the best fit of the experimental data using a symmetric model for the interfacial profile (see the insert in Figure 2). This calculation yields a very narrow interface, 1.5 nm, between mPA and d-PS, which is consistent with the observation that polystyrene and the polyamide were highly immiscible.

In contrast to a PS/mPA blend, Li-SPS and mPA are miscible, and that factor tends to broaden the interface between the as-coated bilayer film and promote mixing at elevated temperatures. The neutron reflectivity spectra for a mPA/d-LiSPS bilayer before and after annealing for 30 min at 140 °C, which is well above the T_g of d-LiSPS, are shown in Figure 3. Because of the favorable interaction between the metal sulfonate and amide groups, at 140 °C where mobility of both polymers is high, the two polymers rapidly mix. As a result, after 30 min at 140 °C, the interfacial width was too broad to be resolved by neutron reflectivity since all the interference fringes in the spectrum were damped out.

In order to better investigate the effects of complexation on interfacial mixing, a lower temperature, 96 °C,

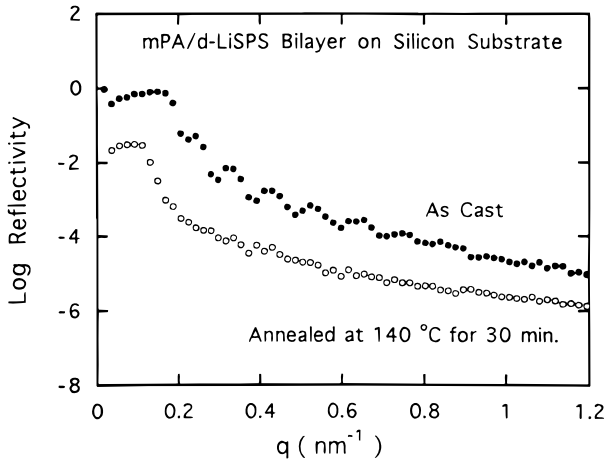

Figure 3. Neutron reflectivity spectra for a mPA/d-LiSPS bilayer on silicon. The filled circles represent the spectrum for the as-cast sample. The empty circles represent the spectrum for a sample annealed at 140 °C for 30 min. The annealed sample data are shifted vertically by log $R = -1.5$ for clarity.

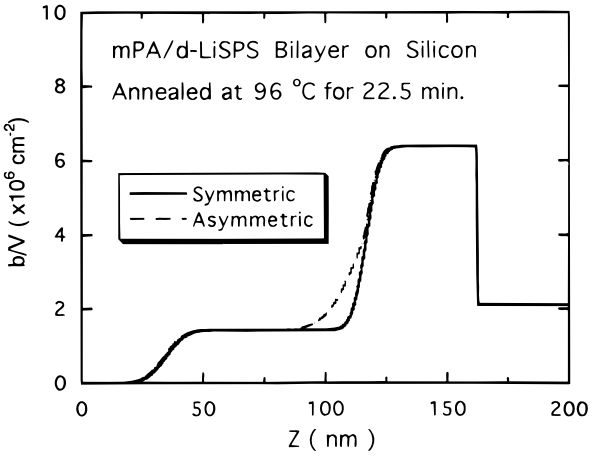

Figure 4. Comparison of the scattering length density profiles predicted by symmetric and asymmetric models for an mPA/d-LiSPS bilayer on silicon annealed for 22.5 min at 96 °C. ($\langle Z_0^2\rangle^{1/2} = 11$ nm, $\langle Z_1^2\rangle^{1/2} = 27$ nm, $\langle Z_2^2\rangle^{1/2} = 11$ nm). The left side of the figure ($Z = 0$) corresponds to air, and the changes in the scattering length density as Z increases correspond to the air/mPA interface, the mPA-rich layer, the mPA/d-LiSPS interface, the d-LiSPS layer, the d-LiSPS/silicon interface, and finally the silicon substrate above $Z = 163$ nm.

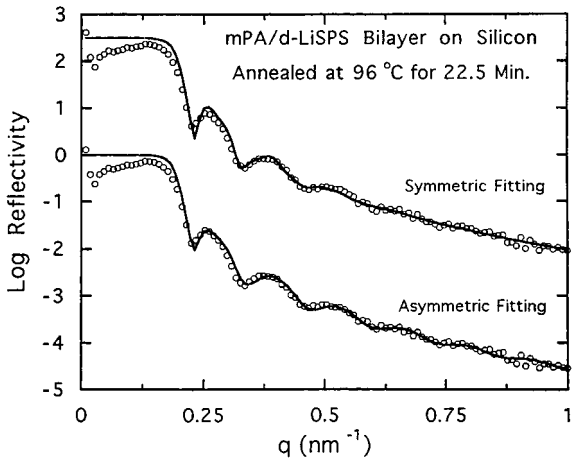

Figure 5. Comparison of the symmetric and asymmetric model fits of the neutron reflectivity of a mPA/d-LiSPS bilayer on silicon substrate annealed for 22.5 min at 96 °C. The curve for the symmetric model fit is shifted vertically by log $R = 2.5$ for clarity.

which is above T_m of mPA but below T_g of the ionomer, was used for further neutron reflectivity experiments. This also necessitated changing the model for the composition profile at the interface, because of the large difference in the molecular mobilities of the polymers at the lower temperature. The symmetric model is usually applicble to the interface between immiscible polymer pairs and for miscible pairs with similar mobilities. However, where there is a large mismatch in the mobilities of the polymers on either side of the interface, as is the case when one polymer is a glass, the composition profile in the interface is not symmetric.[27,47] For the mPA/d-LiSPS bilayer at 96 °C, one expects that the penetration of mPA chains into the glassy d-LiSPS layer would be much slower than penetration of d-LiSPS chains into the mPA melt layer. As a result, an asymmetric interfacial composition profile with a relative sharp interface toward the glassy d-LiSPS layer and a longer tail into the mPA layer is probably more realistic.

To describe the asymmetric interface, we divided the interface into two regions at the position Z where the scattering length density takes the mean value of the two bulk layers. We are only interested in the motion of the mPa/d-LiSPS front, not the specific details of the density profile. The front is defined as the maximum gradient, the motion of which is the second moment of the density distribution. That analysis is relatively insensitive to the specific choice for the density profile.[41] Two Gaussian functions with different values of the characteristic width $\langle Z_1^2\rangle^{1/2}$ and $\langle Z_2^2\rangle^{1/2}$ on either side of the interface were used to account for the asymmetry. $\langle Z_1^2\rangle^{1/2}$ characterizes the interfacial width toward the mPA layer and is larger than $\langle Z_2^2\rangle^{1/2}$, which characterizes the interfacial width toward the d-LiSPS layer. Figure 4 compares the scattering length density profiles predicted by the symmetric and asymmetric models for a mPA/d-LiSPS interface after annealing the bilayer at 96 °C for 22.5 min. The best least-squares fits of the experimental neutron reflectivity data by the two models are shown in Figure 5. Both models fit reasonably well at low q values, but clearly, the asymmetric model is more successful at representing the interface fringe features at high q. For the symmetric model, the reflectivity features are damped out for $q > 0.5$ nm^{-1}. The fitting results shown in Figure 5 are typical of all the analyses performed on all the spectra measured for the mPA/d-LiSPS bilayer annealed at 96 °C, and accordingly, only the asymmetric model fits are used in the following discussion. It should be noted, however, that while the asymmetric model is an improvement over the symmetric model, it is not necessarily the best model or the most accurate representation of the interfacial composition profile. The asymmetryc model is significant only in that within the resolution of these experiments, it suitably represents the general features of the composition profile of the interface.

Figure 6 shows the effect of annealing at 96 °C on the neutron reflectivity spectra for the mPA/d-LiSPS bilayer. The solid lines represent the best fits given by the asymmetric model. The data in Figure 6 yield the following three observations regarding the interfacial mixing in this system: (1) As the annealing (mixing) time increases, the interference fringes of the reflectivity became progressively smeared out, which indicates that the mPA/d-LiSPS interface became progressively broader as a result of interfacial mixing. (2) The critical neutron momentum, q_c, below which total reflection of neutrons occurs, maintained a constant value during the mixing process. Since q_c is determined by the layer with the

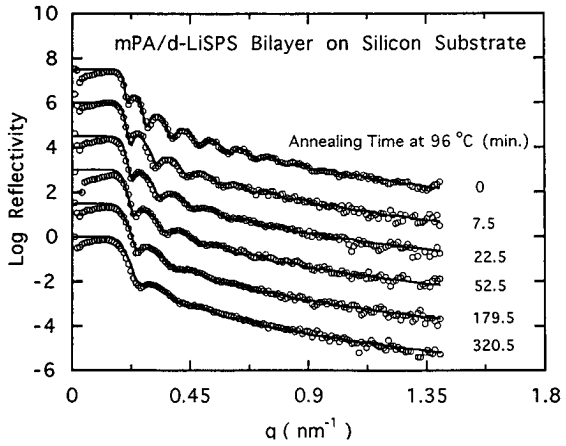

Figure 6. Neutron reflectivity spectra for a mPA/d-LiSPS bilayer on silicon annealed at 96 °C for different times. The solid lines are the best fits of an asymmetric model of the scattering length density profile at the mPA/ionomer interface. For clarity, each curve is shifted log $R = 1.5$ relative to the previous one starting with the data for an annealing time of 320.5 min.

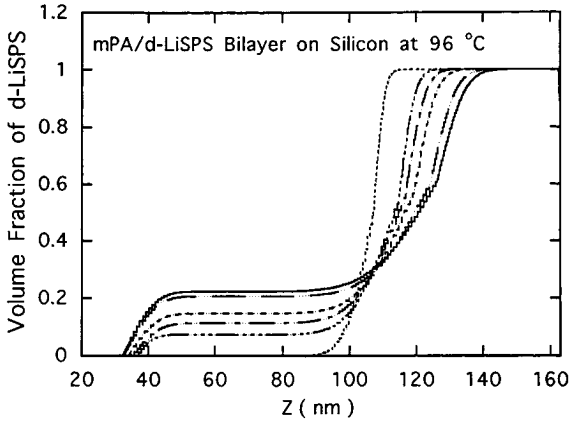

Figure 7. Evolution of the concentration profile at 96 °C for a mPA/d-LiSPS bilayer on silicon. The thicknesses of the d-LiSPS layer and the interfacial profile result from the model fits in Figure 6. The thicknesses of the mPA-rich layer and the volume fraction of d-LiSPS in the mPA-rich layer are calculated from mass conservation.

highest scattering length density, a constant q_c implies that a finite layer of pure d-LiSPS persists throughout the mixing process. (3) The period (Δq) of the interference fringes became progressively larger with annealing time, which signifies a thinning of the d-LiSPS layer. These observations indicate a mixing mechanism for this system in which d-LiSPS chains are depleted from the ionomer layer which broadens the interface with mPA, and this may be accompanied by dissolution of Li-SPS into the bulk of the mPA layer.

Figure 7 gives the temporal evolution of the concentration profiles of d-LiSPS for the mPA/d-LiSPS bilayer annealed at 96 °C. These concentration profiles were the ones used to generate the reflectivity fits in Figure 6. Figure 7 shows that as the polymer/polymer interfacial width increases, the layer of d-LiSPS becomes thinner as a result of its dissolution into the interface. The asymmetry of the interfacial concentration profile is clearly seen in Figure 7, even for the as-coated bilayer. The latter result may be a consequence of the sample preparation in which the mPA solution was directly spun-cast onto the d-LiSPS layer. Although the solvent used for the mPA solution, isopropyl alcohol, is a nonsolvent for d-LiSPS, it may have sufficiently swollen the d-LiSPS surface, increasing its mobility and allowing a finite concentration of mPA to penetrate into the ionomer film.

Ir should be emphasized that the analysis of these reflectivity data is not sensitive to the thickness and composition of the mPA layer. As explained in this paper, the reflectivity data are only sensitive to the thickness of the d-LiSPS layer and the concentration profile of the polymer/polymer interface. Questions such as how much d-LiSPS diffuses into the bulk mPA layer or how thick the mPA-rich layer is cannot be resolved from the data presented herein. Since mass must be conserved, the thickness of the mPA-rich layer and the total concentration of d-LiSPS in that layer may be calculated if it is assumed that the total bilayer thickness does not change appreciably during the mixing process. That calculation, however, cannot determine how the d-LiSPS is distributed in the mPA layer, and although Figure 7 shows a constant concentration profile of d-LiSPS in the mPA-rich layer, this is most likely not the true distribution. In fact, it is more likely that the concentration of d-LiSPS on the mPA side of the interface is more asymmetric than shown in Figure 7. Preliminary forward recoil elastic spectroscopy (FRES) measurements on the longest annealed sample indicated that d-LiSPS did not penetrate completely through the mPA layer to reach the mPA/air interface. Unfortunately, within the resolution of FRES, the detailed profile of the d-LiSPS/mPA interface could not be determined, even for the longest annealing time. Nevertheless, the conclusions reached from the analyses discussed later in this paper are insensitive to the assumptions made about the composition profile on the mPA side of the interface.

As the d-LiSPS dissolves into the mPA layer, the scattering length density of that layer increases. Although this tends to increase the influence of the mPA layer on the reflectivity data, that effect is most likely outweighed by the roughness of the mPA surface and a nonhomogeneous distribution of d-LiSPS in that layer, which obliterate any details of that layer in the reflectivity data. Consequently, a decrease of the differences in scattering length density between the two layers may occur as interfacial mixing proceeds, but the reflectivity details arise mainly from the mPA/d-LiSPS interface and the d-LiSPS layer.

Kinetics of Interfacial Mixing. Two previous studies[27,47] of interfacial mixing in polymer/polymer systems in which one component was a melt and the other a glass are particularly relevant to the present work. Sauer and Walsh[27] used spectroscopic ellipsometry to study interfacial mixing between polystyrene (PS) and poly(vinyl methyl ether) (PVME) at a temperature between the T_g's of the two polymers. They found that the displacement of the PS/PVME interface was linear with annealing time, which corresponds to Case II diffusion; i.e., the mixing kinetics were controlled by the relaxation of the glassy polystyrene. That finding agrees with the mechanism of diffusion of low molecular weight solvents into glassy polymers,[22−26] and it indicates a higher rate of PS diffusion into the PVME layer than vice versa.

In another study, Composto and Kramer[47] used Rutherford backscattering to probe the interfacial mixing between polystyrene and poly(xylenyl ether) (PXE) at several temperatures between the T_g's of the pure polymers. They observed that mixing proceeded with a thinning of the PXE layer and the displacement of the interface scaled as $t^{1/2}$. The later observation indicates Fickian diffusion. Additionally, the concentration profile across the interface was asymmetric, quali-

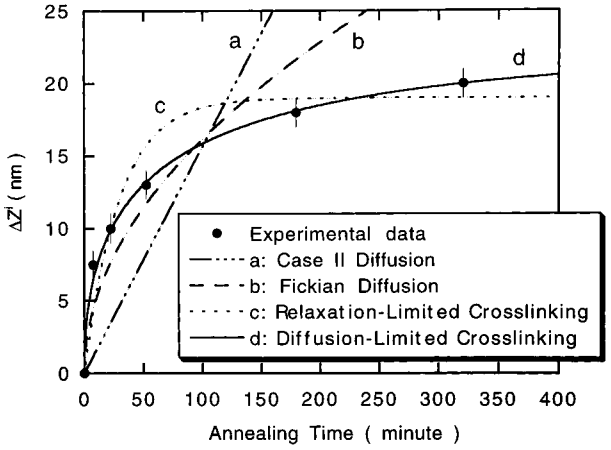

Figure 8. Displacement of the d-LiSPS layer front at 96 °C as a function of annealing time for a mPA/d-LiSPS bilayer on silicon. The filled circles are calculated from the asymmetric concentration profile fits in Figure 7. The curves are predictions of different kinetic models: (a) Case II diffusion ($\Delta Z^i = kt$); (b) Fickian diffusion ($\Delta Z^i = kt^{1/2}$); (c) relaxation-controlled cross-linking (eq 4 in text); (d) diffusion-controlled cross-linking (eq 5 in text).

tatively similar to what was reported herein for the mPA/d-LiSPS system.

Similar to the above cases, the displacement of the mPA/d-LiSPS interface in the present study was also toward the glassy layer as shown in Figure 7. The position, Z^i, of the interface is defined by the maximum slope in the d-LiSPS concentration profile, and the shift (ΔZ^i) at any time is taken relative to the interface position at $t = 0$. Figure 8 plots ΔZ^i as a function of annealing time at 96 °C for the mPA/d-LiSPS bilayer. Lines a and b in Figure 8 correspond to Case II($\Delta Z^i \sim t$) and Fickian diffusion ($\Delta Z^i \sim t^{1/2}$), respectively. Clearly the kinetics of the interface displacement in this system follows neither a linear nor a square-root relationship with time, which indicates that the mixing process cannot be described solely by polymer relaxation or simple molecular diffusion.

Figure 8 shows that the interfacial mixing occurs rapidly at short times but then gradually slows down to less than the $t^{1/2}$ relationship of a pure diffusion mechanism and appears to asymptote toward a fixed interface at long times. One explanation for the slowing down of the interface displacement is the formation of intermolecular complexes at the interface which produces a physically cross-linked network. As mentioned earlier, this particular blend exhibits very strong specific attractive interactions between the metal sulfonate and amide groups. The specific nature of those interactions is discussed in a previous paper.[39] When the effective molecular weight of this cross-linked network becomes high enough, the entire interfacial mixing process stalls because of the lack of chain mobility, although, of course, thermodynamics still favor further mixing.

To account for the effect of intermolecular complexation on the mixing kinetics, we added a term for cross-linking into the two conventional diffusion models described earlier. As discussed above, interfacial mixing of d-LiSPS/mPA at 96 °C involves dissolution of d-LiSPS chains into the mPA layer. Concurrent with mixing is the formation of a physical network between the polyamide and the ionomer. If we assume steady-state dynamics, the rate of the cross-linking reaction is identical to the rate of dissolution of d-LiSPS into the interfacial region. A boundary condition on the cross-linking reaction is that as $t \rightarrow \infty$, the total number of cross-link junctions, n, is $n_\infty = \rho_c V_\infty$, where ρ_c is the cross-link density, which is proportional to the sulfonation level of d-LiSPS, and V_∞ is the total volume of d-LiSPS that is cross-linked at $t \rightarrow \infty$. The interface displacement, $\Delta Z^i(t)$, is assumed to be proportional to $V(t)$, the volume of d-LiSPS that has been dissolved or complexed at t.

In the first case, the cross-linking mechanism is combined with the Case II diffusion mechanism. In this case, interdiffusion is fast and the cross-linking rate, $dn(t)/dt$ depends only on how many uncross-linked junctions remain $[n_\infty - n(t)]$,

$$\frac{dn(t)}{dt} = k[n_\infty - n(t)] \tag{2}$$

In the second case, the cross-linking reaction is combined with a simple, diffusion-limited mixing mechanism. In this case, the cross-linking rate not only depends on how many uncross-linked junctions remain but also on how rapidly the d-Li SPS diffuses to the polyamide. For Fickian diffusion,[7] the volume flux per unit concentration across a flat plane is $R(t) = \sqrt{D/\pi t}$, and when this is combined with the cross-linking equation, the rate of cross-linking becomes

$$\frac{dn(t)}{dt} = k(D/\pi t)^{1/2}\rho[n_\infty - n(t)] \tag{3}$$

In the latter derivation, the effect of cross-linking on $R(t)$ was neglected, and therefore, 3 represents only a first-order approximation of the cross-linking kinetics. That is, it assumes that the available number of cross-linkable junctions at any given time is simply the remaining number of junctions, $(n_\infty - n(t))$, multiplied by the rate of transportation to the reaction sites by diffusion. A similar argument was recently made for surface-limited diffusion in polymer adsorption and desorption from solution,[48,49] and this kinetics is expected to be generic for similar phenomena.

Since $(n(t) = \rho_c v(t)$, $v(t)$ is proportional to $\Delta Z^i(t)$, and with the initial condition of $\Delta Z^i(0) = 0$, the solutions to eqs 2 and 3 are, respectively,

$$\Delta Z^i(t) = \Delta Z_\infty[1 - \exp(-t/t_0)] \tag{4}$$

$$\Delta Z^i(t) = \Delta Z_\infty[1 - \exp(-(t/t_0)^{1/2})] \tag{5}$$

where ΔZ^i_∞ and t_0 are constants for a given system at a given temperature. Equation 4, which represents the case where the overall kinetics of mixing are dominated by the relaxation of the glassy Li-SPS, predicts that the displacement of the interface follows a simple exponential relationship with time. Equation 5, which we call the *diffusion-limited cross-linking* (DLC) mechanism, predicts a stretched exponential relationship with time appearing as the $^1/_2$ power.

In Figure 8, lines c and d correspond to the relaxation-controlled and diffusion-limited cross-linking mechanisms, eqs 4 and 5, respectively. The agreement of the DLC model with the experimental data is quite good. For early times, the DLC model predicts a $t^{1/2}$ relationship for the interface displacement, which implies diffusion-controlled kinetics at the beginning of the mixing process. As mixing proceeds, however, diffusion is suppressed by intermolecular complexation. The formation of a physically cross-linked network is also supported by FRES measurements. When the longest annealed sample was further annealed for an additional

2 days, FRES indicated that the position of the d-LiSPS/mPA interface did not shift significantly.

Similar diffusion-limited kinetics have been reported for polymer adsorption and desorption.[48,49] In those studies, the kinetics of desorption and adsorption of a polymer layer at a planar surface showed a transition from simple exponential kinetics at high temperatures where diffusion of the polymer was faster than the activated rate processes of adsorption or desorption to stretched-exponential kinetics at lower temperatures where the adsorption or desorption processes became diffusion-limited.

The question of whether a similar transition in the kinetics for interfacial mixing of the mPA/d-LiSPS system occurs at higher temperatures is an intriguing one that will be pursued in future studies. On the one hand, one might expect that at temperatures above the T_g's of both polymers, the cross-linking reaction will control the interfacial mixing, which would also yield exponential kinetics. On the other hand, the stability of the intermolecular complex is also temperature dependent, and the cross-linking mechanism may diminish in importance as the complex becomes weaker. The strength of the intermolecular complex and its temperature dependence may also be varied by changing the counterion used to neutralize the ionomer.[36,38,39] For example, ZnSPS forms a stronger and more temperature-resistant complex with polyamides, and further studies using ZnSPS are planned.

Conclusions

The introduction of lithium−sulfonate groups into polystyrene has a marked influence on the interface characteristics with a model polyamide, poly(*N*,*N*′-dimethylethylenesebacamide), which is immiscible with polystyrene. At 96 °C, a temperature below the T_g of the ionomer and above the T_m of the polyamide, the concentration profile across the LiSPS/mPA interface is asymmetric with a relatively steeper slope on the glassy ionomer side of the interface and a relatively long tail toward the polyamide layer. The mixing kinetics initially follows a $t^{1/2}$ dependence, consistent with Fickian diffusion, but exhibits a slowing down as the process continues. A diffusion-limited mixing model based on a combinatin of Fickian diffusion and physical cross-linking adequately accounted for the observed mixing behavior in this system and may have general application to mixing in polymer blends exhibiting strong intermolecular interactions.

Acknowledgment. This research was supported by the Polymer Compatibilization Research Consortium at the University of Connecticut and by a grant from the Polymer Program of the National Science Foundation (Grant DMR 9400862). Useful discussions with Dr. J. Douglas of NIST are also greatly appreciated.

References and Notes

(1) Ting, S. P.; Pearce, E. M.; Kwei, T. K. *J. Polym. Sci., Polym. Lett. Ed.* **1980**, *18*, 201.
(2) Kwei, T. K.; Pearch, E. M.; Min, B. Y. *Macromolecules* **1985**, *18*, 2326.
(3) Prud'homme, R. E. *Polym. Eng. Sci.* **1982**, *22*, 90.
(4) Hara, M.; Eisenberg, A. *Macromolecules* **1984**, *17*, 1335.
(5) Sen, A.; Weiss, R. A.; Garton, A. In *Multiphase Polymer: Blends and Ionomers;* Utracki, L. A., Weiss, R. A., Eds.; ACS Symposium Series 395; American Chemical Society: Washington, DC, 1989.
(6) Natansohn, A.; Murali, R.; Eisenberg, A. *ChemTech* **1990**, July, 418.
(7) Lu, X.; Weiss, R. A. *Mat. Res. Soc. Symp.* **1991**, *215*, 29.
(8) Lu, X.; Weiss, R. A. *Macromolecules* **1992**, *25*, 6185.
(9) Paul, D. R., Newman, S., Eds. *Polymer Blends*; Academic: New York, 1978; Vols. I and II.
(10) Paul, D. R., Sperling, L. H., Eds. *Multicomponent Polymer Materials*; Advances in Chemsitry Series 211; American Chemical Society: Washington, DC, 1986.
(11) Kausch, H. H.; Tirrell, M. *Annu. Rev. Mater. Sci.* **1989**, *19*, 341.
(12) Jabbari, E.; Peppas, N. A. *J. M. S.-Rev. Macromol. Chem. Phys.* **1994**, *C34* (2), 205.
(13) Voyutskii, S. S. *J. Adhes.* **1971**, *3*, 69.
(14) de Gennes, P. G. *C. R. Acad. Sci. Paris, Ser. II* **1981**, *292*, 1505.
(15) Crank, J. *The Mathematics of Diffusion*; Claredon: Oxford, 1956.
(16) Brochard, B.; de Gennes, P. G. *Phys. Chem. Hydrodynam.* **1983**, *4*, 313.
(17) Brochard, B.; de Gennes, P. G. *Europhys. Lett.* **1986**, *1* (5), 211.
(18) Kramer, E. J.; Green, P. F.; Palmstrøm, C. J. *Polymer* **1984**, *25*, 473.
(19) Green, P. F.; Palmstrøm, C. J.; Mayer, J. W.; Kramer, E. J. *Macromolecules* **1985**, *18*, 501.
(20) Fernandez, M. L.; Higgins, J. S.; Penfold, J.; Shackleton, C. *J. Chem. Soc., Faraday Trans.* **1991**, *87* (13), 2055.
(21) Hopfenberg, H. B.; Stannett, V. T. in *The Physica of Glassy Polymers*; Haward, R. N., Eds.; Wiley: New York, 1973; Chapter 9.
(22) Alfrey, T., Jr.; Gurnee, E. F.; Lloyd, W. G. *J. Polym. Sci.* (C), **1966**, *12*, 249.
(23) Enscore, D.J.; Hopfenberg, H. B.; Stannett, V. T. *Polymer*, **1977**, *18*, 793.
(24) Gall, T. P.; Lasky, R. C.; Kramer, E. J. *Polymer* **1990**, *31*, 1491.
(25) Gall, T. P.; Kramer, E. J. *Polymer* **1991**, *32*, 265.
(26) Mills, P. J.; Kramer, E. J. *J. Mater. Sci.* **1986**, *21*, 4151.
(27) Sauer, B. B.; Walsh, D. J. *Macromolecules* **1991**, *24*, 5948.
(28) Jabbari, E.; Peppas, N. A. *Macromolecules* **1993**, *26*, 2175.
(29) Huang, S. J.; Kozakiewicz, J. *J. Macromol. Sci.-Chem.* **1981**, *A15*, 821.
(30) Madan, S. K.; Sturr, J. A. *J. Inorg. Nucl. Chem.* **1967**, *29*, 1669.
(31) Balasubramanian, D.; Shaikh, R. *Biopolymers* **1973**, *12*, 1639.
(32) Madan, S. K.; Sturr, J. A. *J. Inorg. Nucl. Chem.* **1967**, *29*, 1669.
(33) Bull, W. E.; Madan, S. K.; Willis, J. E. *Inorg. Chem.* **1963**, *2*, 303.
(34) Dunn, P.; Sansom, G. F. *J. Appl. Polym. Sci.* **1969**, *13*, 1657.
(35) Roberts, M. F.; Jenekhe, S. A. *Macromolecules* **1991**, *24*, 3142.
(36) Weiss, R. A.; Lu, X. *Polymer* **1994**, *35*, 1963.
(37) Rajagopalan, P.; Kim, J.-S.; Brack, H. P.; Lu, X.; Eisenberg, A.; Weiss, R. A.; Risen, W. M., Jr. *J. Polym. Sci., Polym. Phys.* **1995**, *33*, 495.
(38) Feng, Y. Ph.D. Thesis, University of Connecticut, 1995.
(39) Feng, Y.; Schmidt, A.; Weiss, R. A. *Macromolecules* **1996**, *29*, 3909.
(40) Russell, T. P. *Mater. Sci. Rep.* **1990**, *5*, 171.
(41) Karim, A.; Mansour, A.; Felcher, G. P.; Russell, T. P. *Phys. Rew. B* **1990**, *42*, 6846; *Macromolecules* **1994**, *27*, 6973.
(42) Fernandez, M. L.; Higgins, J. S.; Penfold, J.; Ward, R. C.; Shackleton, C.; Walsh, D. J. *Polymer* **1990**, *31*, 2174.
(43) Makowski, H. S.; Lundberg, R. D.; Singhal, G. H. U.S. Patent 3870841, 1975.
(44) Shibayama, M.; Yang, H.; Stein, R. S.; Han, C. C. *Macromolecules* **1985**, *18*, 2179.
(45) Weiss, R. A.; Lundberg, R. D.; Turner, S. R. *J. Polym. Sci., Polym. Chem. Ed.* **1985**, *23*, 549.
(46) Ankner, J. F. In *Surface X-Ray and Neutron Scattering*; Springer Proceedings in Physics; Springer: New York, 1992; Vol. 61, p 105.
(47) Composto, R. J.; Kramer, E. J., *J. Mater. Sci.* **1991**, *26*, 2815.
(48) Douglas, J. F.; Johnson, H. E.; Granick, S. *Science* **1993**, *262*, 2010.
(49) Douglas, J. F.; Frantz, P.; Johnson, H. E.; Schneider, H. M.; Granick, S. *Colloids Surf. A* **1994**, *86*, 251.

MA951723J